Jordan Journal of Civil Engineering, Volume **11**, No. **2**, **2017**

A Hybrid Magnetic CSS and BBBC for Optimum Design of Double Curvature Arch Dams

Reza Parsiavash [1)]***, Mohammad Taghi Alami*** [2)] ***and Siamak Talatahari*** [3)]

[1)] University of Tabriz, Iran. E-Mail: rparsiavash@gmail.com
[2)] University of Tabriz, Iran. E-Mail: taalami@tabrizu.ac.ir
[3)] University of Tabriz, Iran. E-Mail: siamak.talat@gmail.com

ABSTRACT

This paper presents a hybrid metaheuristic approach to find the optimal shape of double curvature arch dams, considering dam-reservoir interaction and hydrodynamic effects under time-history seismic analysis. Magnetic charged system search and big bang-big crunch are utilized to present a hybrid method. A real-world arch dam is considered as a numerical example to demonstrate the efficiency of the proposed method. Results obtained from this study are compared to those reported in literature. The results show that the new method yields better performance and is more effective compared to its rivals.

KEYWORDS: Magnetic charged system search, Big bang-big crunch, Double curvature arch dam, Optimum design, Dam-reservoir interaction.

INTRODUCTION

The geometry of a double curvature arch dam has a great influence on its safety and economy. Recent developments in the field of optimization techniques have led to a renewed interest in finding the optimal design of arch dams. Generally, the objective is to find the optimal shape with minimum concrete volume subjected to geometric, stability and behavioral constraints. This problem is known as a non-linear and non-convex one.

From structural behavior point of view, the fluid-structure interaction under seismic loads is of high importance in the arch dam. Earthquake acceleration produces not only dynamic loads on the dam body, but also hydrodynamic pressures in the reservoir, which, in turn, intensifies resultant stresses on the arch dam due to dam-reservoir interaction effects. Despite this, to avoid the complexity of the problem, some simplifications are involved in recent works. In a number of studies, the arch dam is considered with an empty reservoir (Kaveh and Mahdavi, 2011; Gholizadeh and Seyedpoor, 2011) and in some other studies, the reservoir's effect is simplified by added mass approach (Kaveh and Mahdavi, 2014; Akbari et al., 2011), which overestimates the hydrodynamic effects in the dam body (Kuo, 1982). Recently, charged system search (CSS) is proposed by Kaveh and Talatahari (2010 a) that is suitable for non-convex problems and many successful applications of it have been reported in literature (Kaveh and Talatahari, 2010 b; Kaveh and Talatahari, 2012 a; Kaveh et al., 2012 b). The CSS utilizes the Coulomb and Gauss's laws from electrostatics and Newtonian laws of mechanics. The magnetic charged system search (MCSS) (Kaveh et al., 2013) is an improved version of the CSS, in which magnetic forces are considered in addition to electrical forces using the Biot-Savart law

Received on 22/9/2015.
Accepted for Publication on 8/12/2016.

(Halliday et al., 2008). This additional force provides useful information for the optimization process and enhances the performance of the CSS algorithm (Kaveh et al., 2013). Big Bang-Big Crunch (BBBC) is another metaheuristic approach that is based on one of the theories of evolution of the universe with the same name (Erol and Eksin, 2006).

In this study, an efficient methodology is presented to find the optimal shape of double curvature arch dams, considering hydrodynamic effects. The optimization task is performed using a hybridized MCSS-BBBC method. The concrete volume of the dam body is considered as the objective function and the geometrical parameters will be its design variables. The constraints are enforcing stress state to meet Willam-Warnke failure criterion as well as some geometric and stability constraints. The effectiveness of the proposed methodology is then evaluated for a well-known benchmark arch dam and compared to other meta-heuristic methods documented in literature.

GEOMETRICAL MODEL OF AN ARCH DAM

Shape of the Central Vertical Section

The shape of a double-curvature arch dam has two basic characteristics: curvature and thickness. Both curvature and thickness change in horizontal and vertical directions. For the central vertical section of a double-curvature arch dam, as shown in Fig. 1, one polynomial of n^{th} order is used to determine the curve of the upstream boundary and another polynomial is employed to determine the thickness. In this study, a parabolic function is considered for the curve of upstream face as (Gholizadeh and Seyedpoor, 2011):

$$g(z)=\frac{\gamma z^{2}}{2\beta h}-\gamma z \tag{1}$$

where h and γ are the height of the dam and the slope at crest, respectively, and the point where the slope of the upstream face equals zero is $z = \beta h$, in which β is constant as shown in Fig.1.

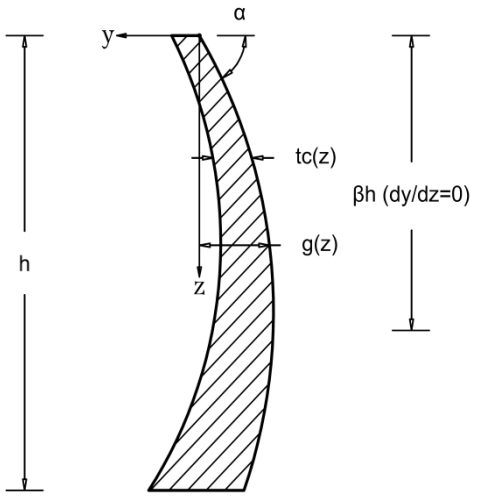

Figure (1): Crown cantilever profile of the arch dam

By dividing the height of dam into n equal segments containing n + 1 levels, the thickness of the central vertical section can be expressed as:

$$t_c(z)=\sum_{i=1}^{n+1}L_i(z)t_{ci} \tag{2}$$

in which, t_{ci} is the thickness of the central vertical section at the i^{th} level. Also, in the above relation, $L_i(z)$ is a Lagrange interpolation function associated with the i^{th} level and can be defined as:

$$L_i(z)=\prod_{\substack{m=1\\ m\neq i}}^{n+1}\frac{z-z_m}{z_i-z_m} \tag{3}$$

where z_i and z_m denote the z coordinate of the i^{th} and m^{th} level in the central vertical section, respectively.

Shape of the Horizontal Section

As shown in Fig. 2, for the purpose of symmetrical canyon and arch thickening from crown to abutment, the shape of the horizontal section of a parabolic arch dam is determined by the following two parabolas:

$$y_u(x,z)=\frac{x^{2}}{2r_u(z)}+g(z) \tag{4}$$

$$y_d(x,z) = \frac{x^2}{2r_d(z)} + g(z) + t_c(z) \quad (5)$$

$$r_u(z) = \sum_{i=1}^{n+1} L_i(z)\, r_{ui} \quad (6)$$

$$r_d(z) = \sum_{i=1}^{n+1} L_i(z)\, r_{di} \quad (7)$$

where y_u *(x, z)* and y_d *(x, z)* are parabolas of the upstream and downstream faces, respectively. r_u and r_d are the radii of curvatures corresponding to upstream and downstream curves, respectively, and functions of n^{th} order with respect to z can be used for those radii:

where r_{ui} and r_{di} are the values of r_u and r_d at the i^{th} level, respectively.

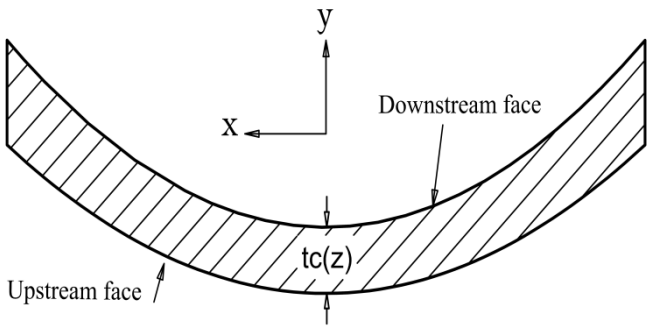

Figure (2): Parabolic shape of an elevation of the arch dam

FINITE ELEMENT MODEL OF AN ARCH DAM

The Morrow point double curvature arch dam is analyzed to assist the validation of the finite element model utilized in this study. This dam has been studied by many researchers, so that the results of our study can be verified with already published material. This dam is located on the Gunnison River in Montrose Country near the village of Cimarron, Colorado. The dam is 142.65 m high and 220.68 m long along the crest and its thickness varies from 3.66 m at the crest to 15.85 m at the base level. The geometric properties of the dam in detail can be found in USACE (2007). The physical and mechanical properties involved here are the concrete density (2483 $N.s^2/m^4$), the concrete Poisson's ratio (0.2) and the concrete elasticity (27580 MPa). In this analysis, the hydrodynamic effects of dam-reservoir interaction are considered. The dam body is discretized with two hundred and eighty 8-node solid elements including 495 nodes for the dam body and one thousand and four hundred 8-node fluid elements including 2145 nodes for the reservoir. This number of nodes and elements is not constant during the optimization process due to changes in the dimensions of the arch dam and mesh generation in every analysis, so it will be varied when needed. The arch dam is analyzed as a 3D-linear structure and the natural frequencies from the literature and the present work are provided in Table 1. It can be observed that a good conformity has been achieved between the results of the present work and those reported in the literature.

ARCH DAM OPTIMIZATION

Mathematical Model and Optimization Variables

The optimization problem can formally be stated as follows:

Find: $\boldsymbol{X} = [x_1, x_2, x_3, ..., x_n]$ (8)

(*Minimize:* $Mer(\boldsymbol{X}) = f(\boldsymbol{X}) * f_{penalty}(\boldsymbol{X})$ (9)

$$\text{Subject to:} \quad g_i(\boldsymbol{X}) \le 0, \quad i = 1,2,...,\text{k} \qquad (10)$$
$$x_{i\min} \le x_i \le x_{i\max}$$

where $\boldsymbol{X}$ is the vector of design variables with n unknowns, g_i is the i^{th} constraint from k inequality constraints and *Mer* $(\boldsymbol{X})$ is the merit function. $f(\boldsymbol{X})$ is the objective function which is generally to minimize the construction cost of the dam. A combination of concrete volume and casting area of the dam body can be considered as the objective function. However, since the variation of casting area between various designs is negligible (about one percent), it can be omitted in the optimization process. So, in this study, just the concrete volume of the dam is considered as the objective function:

$$v(\boldsymbol{X}) = \iint_A \left| y_u(x,z) - y_d(x,z) \right| dA \qquad (11)$$

in which, A is an area produced by projecting the dam on the xz plane. In Eq. (9), $f_{penalty}(\boldsymbol{X})$ is the penalty function which results from the violations of the constraints corresponding to the response of the arch dam. Also, $x_{i\,min}$ and $x_{i\,max}$ are the lower and upper bounds of design variable vector. Exterior penalty function method is employed to transform the constrained dam optimization problem into an unconstrained one as follows:

$$f_{penalty}(\boldsymbol{X}) = 1 + \gamma_p \sum_{i=1}^{k} \max(0, gj(\boldsymbol{X}))^2 \qquad (12)$$

where y_p is the penalty multiplier.

Design Variables

The most effective parameters for creating the arch dam geometry were previously mentioned. These parameters can be adopted as design variables:

$$\boldsymbol{X} = \{\gamma \quad \beta \quad tc_1 \ldots tc_{n+1} \quad ru_1 \ldots ru_{n+1} \quad rd_1 \ldots rd_{n+1}\} \qquad (13)$$

in which, $\boldsymbol{X}$ contains 2+3 (n+1) shape parameters of the arch dam, where n is the number of divisions along the dam height.

Table 1. Comparison of natural frequencies from the literature with FEM

Mode	(Tan and Chopra, 1996)		(Duron and Hall, 1988)		Present work	
	empty	full	full		empty	full
	FEA		FEA	experimental	FEA	
1	4.27	2.82	3.05	2.95	4.2897	2.9607
2	-	-	-	3.3	-	3.3046
3	-	-	4.21	3.95	-	4.2425
4	-	-	5.96	5.4	-	4.9522
5	-	-	-	6.21	-	6.1156

Design Constraints

Design constraints are divided into some groups, including behavioral, geometrical and stability constraints. In most of the existing studies, the separate restrictions of the principal stresses were considered as behavior constraints. In this study, the behavior constraints are defined to prevent the crash and crack of each element (e) of the arch dam under specified safety factor (s_f) in all time points of the specified earthquake. For this purpose, the failure criterion of concrete of Willam and Warnke (1975) due to a multi-axial stress state is employed. Thus, time-dependent (t) behavior constraints for the dam body are expressed as:

$$\left(\frac{F}{f_c}\right)_{e,t} \le \left(\frac{S}{s_f}\right)_{e,t} \Rightarrow gbe(x,t) = \left(\frac{F}{f_c} - \frac{S}{s_f}\right)_{e,t} \le 0, e = 1,2,..,n_e, t = 1,2,..,T \qquad (14)$$

where F is function of the principal stress state ($\sigma_1 \ge \sigma_2 \ge \sigma_3$) and S is the failure surface expressed in terms of principal stresses containing uniaxial compressive strength of concrete (f_c), uniaxial tensile strength of concrete (f_t) and biaxial compressive strength of concrete (f_{cb}). T is the earthquake duration. According

to the four principal stress states: compression - compression - compression, tensile-compression-compression, tensile-tensile-compression and tensile-tensile-tensile, the failure of concrete is categorized into four domains. In each domain, independent functions describe F and the failure surface S. For instance, in the compression-compression-compression regime, F and S are defined as:

$$F = \frac{1}{\sqrt{15}}\left[\left(\sigma_1-\sigma_2\right)^2+\left(\sigma_2-\sigma_3\right)^2+\left(\sigma_3-\sigma_1\right)^2\right]^{\frac{1}{2}} \quad (15)$$

$$S = \frac{2r_2\left(r_2^2-r_1^2\right)\cos\eta + r_2\left(2r_1-r_2\right)\left[4\left(r_2^2-r_1^2\right)\cos^2\eta+5r_1^2-4r_1r_2\right]^{\frac{1}{2}}}{4\left(r_2^2-r_1^2\right)\cos^2\eta+\left(r_{2-}2r_1\right)^2} \quad (16)$$

where the angle of similarity $0 \le \eta \le 60$ describes the relative magnitudes of the principal stresses as:

$$\cos\eta = \frac{2\sigma_1-\sigma_2-\sigma_3}{\sqrt{2}\left[\left(\sigma_1-\sigma_2\right)^2+\left(\sigma_2-\sigma_3\right)^2+\left(\sigma_3-\sigma_1\right)^2\right]^{\frac{1}{2}}} \quad (17)$$

The parameters r_1 and r_2 represent the failure surface of all the stress states with η = 0 and η = 60, respectively, and these are functions of the principal stresses and concrete strengths (f_c, f_t, f_{cb}). The details of the failure criterion can be found in Willam and Warnke (1975). Therefore, Eq. (14) is checked at the center of all dam elements (*ne*) for the earthquake loading (USBR, 1977). If it is satisfied, there is no cracking or crushing. Otherwise, the material will crack if any principal stress is tensile, while crushing will occur if all principal stresses are compressive. The most important geometrical constraints are those that prevent from intersection of upstream face and downstream face, as:

$$r_{di} \le r_{ui} \Rightarrow \frac{r_{di}}{r_{ui}} - 1 \le 0, i = 1,2,...,(n+1) \quad (18)$$

where r_{di} and r_{ui} are the radii of curvatures at the downstream and upstream faces of the dam at the i^{th} level in the z direction, respectively and n is the number of divisions along the dam height. The geometrical constraint that is applied to facilitate the construction is defined as:

$$\gamma \le \gamma_{alw} \Rightarrow \frac{\gamma}{\gamma_{alw}} - 1 \le 0 \quad (19)$$

where γ is the slope of overhang at the downstream and upstream faces of the dam and γ_{alw} is its allowable value. Usually, γ_{alw} is taken as 0.3 (Zhu et al., 1992).

OPTIMIZATION ALGORITHMS

As mentioned before, in this paper, a powerful advanced algorithm consisting of the magnetic CSS and the standard BBBC is employed for optimal design of arch dams. Therefore, in the following part, we will firstly describe the standard and magnetic CSS-based methods as well as the BBBC and then MCSS-BBBC is introduced by combining these methods.

The Standard Charged Search System

The CSS (Kaveh and Talatahari, 2010 a) is a population-based search approach which is based on principles from physics and mechanics. In this approach, each agent is a charged particle (CP) which is considered as a charged sphere of radius a, having a uniform volume charge density that can produce an electric force on the other CPs. The force magnitude for a CP located inside the sphere is proportional to the separation distance between the CPs, while for a CP located outside the sphere it is inversely proportional to the square of the separation distance between the particles. The resultant forces or acceleration and the motion laws determine the new location of the CPs. The pseudo-code for the CSS algorithm can be summarized as follows (Kaveh and Talatahari, 2010 b):

Step 1: *Initialization.* The initial positions of CPs are randomly determined in the search space and the initial velocities of CPs are assumed to be zero. The values of the fitness function for the CPs are determined and the CPs are sorted in an increasing order. A number of the first CPs and their related values of the fitness function are saved in a memory, called the Charged Memory (CM).

Step 2: *Determination of the forces on CPs.* The force vector is calculated for the j^{th} CP as:

$$\boldsymbol{F}_j = \sum_{i,i\neq j}\left(\frac{q_i}{a^3}r_{ij}\cdot i_1+\frac{q_i}{r_{ij}^2}\cdot i_2\right)ar_{ij}\,p_{ij}(\boldsymbol{X}_i-\boldsymbol{X}_j)\begin{cases} j=1,2,...,N \\ i_1=1,i_2=0\Leftrightarrow r_{ij}<a \\ i_1=0,i_2=1\Leftrightarrow r_{ij}\geq a\end{cases} \quad (20)$$

where F_j is the resultant force acting on the j^{th} CP. $\boldsymbol{X}_i$ and $\boldsymbol{X}_j$ are the position vectors of the i^{th} and j^{th} CPs, respectively. Here, a is the radius of the charged sphere and N is the number of CPs. The magnitude of charge for each CP (q_i) is defined considering the quality of its solution as:

$$q_i=\frac{fit(i)-fitworst}{fitbest-fitworst},\qquad i=1,2,\ldots,N \quad (21)$$

where *fitbest* and *fitworst* are the best and worst fitness of all particles, respectively, *fit(i)* represents the fitness of the agent i and N is the total number of CPs. The separation distance r_{ij} between two charged particles is defined as follows:

$$r_{ij}=\frac{\|\boldsymbol{X}_i-\boldsymbol{X}_j\|}{\|(\boldsymbol{X}_i+\boldsymbol{X}_j)/2-\boldsymbol{X}_{best}\|+\varepsilon} \quad (22)$$

where $\mathbf{X}_{best}$ is the position of the best current CP and ε is a small positive number. Here, p_{ij} is the probability of moving each CP towards the others and is obtained using the following function:

$$p_{ij}=\begin{cases}1 & \frac{fit(i)-fitbest}{fit(j)-fit(i)}>rand\vee fit(i)>fit(j)\\ 0 & \text{else}\end{cases} \quad (23)$$

In Eq. (20), ar_{ij} indicates the kind of force and is defined as:

$$ar_{ij}=\begin{cases}+1 & rand<0.8\\ -1 & else\end{cases} \quad (24)$$

where *rand* represents a random number.

Step 3: *Solution construction.* Each CP moves to the new position and the new velocity is calculated as:

$$\boldsymbol{X}_{j,new}=rand_{j1}\cdot k_a\cdot\boldsymbol{F}_j+rand_{j2}\cdot k_v\cdot\boldsymbol{V}_{j,old}+\boldsymbol{X}_{j,old} \quad (25)$$

$$\boldsymbol{V}_{j,new}=\boldsymbol{X}_{j,new}-\boldsymbol{X}_{j,old} \quad (26)$$

where k_a is the acceleration coefficient, k_v is the velocity coefficient to control the influence of the previous velocity and $rand_{j1}$ and $rand_{j2}$ are two random numbers uniformly distributed in the range (0,1). In this paper, k_a and k_v are taken as:

$$k_a=0.5\left(1+\frac{iter}{iter_{\max}}\right),k_v=0.5\left(1-\frac{iter}{iter_{\max}}\right) \quad (27)$$

where *iter* is the iteration number and $iter_{max}$ is the maximum number of iterations.

Step 4: *Updating process.* If a new CP exits from the allowable search space, a harmony search-based handling approach is used to correct its position. In addition, if some new CP vectors are better than the worst ones in the CM, these are replaced by the worst ones in the CM.

Step 5: *Termination criterion control.* Steps 2-4 are repeated until a termination criterion is satisfied (Kaveh and Talatahari, 2010 a).

Magnetic Charged System Search Algorithm

The main structure of the algorithm is the same as the standard CSS, but with some modification in the part of the algorithm where the forces are computed. Thus, for considering this force in addition to electric force, the CSS algorithm is extended to the MCSS algorithm by Kaveh et al. (2013). In the MCSS algorithm, all steps described for the CSS are valid, yet; however, the relationship for the force affecting each CP should be modified considering the magnetic fields.

$$\boldsymbol{F}=p_r*\boldsymbol{F}_E+\boldsymbol{F}_B \quad (28)$$

where p_r is the probability that an electrical force is a repelling force. Here, F_E and F_B are the resultant electrical and magnetic forces, respectively. By using Eq. (20), the resultant electrical force acting on the j^{th} CP can be calculated and the magnetic force $F_{B,j}$ acting on the j^{th} CP due to the magnetic field produced by the i^{th} virtual wire (i^{th} CP) can be expressed as:

$$\boldsymbol{F}_{\mathbf{B},j} = q_j \cdot \sum_{i,i\neq j}\left(\frac{I_i}{R^2} r_{ij} \cdot z_1 + \frac{I_i}{r_{ij}} \cdot z_2\right) \cdot pm_{ji} \cdot (\boldsymbol{X}_i - \boldsymbol{X}_j), \begin{cases} z_1 = 1, z_2 = 0 \Leftrightarrow r_{ij} < R, \\ z_1 = 0, z_2 = 1 \Leftrightarrow r_{ij} \geq R, \\ j = 1,2,...,N, \end{cases} \quad (29)$$

where R is the radius of the virtual wires, I_i is the average electric current in each wire and pm_{ji} is the probability of the magnetic influence (attracting or repelling) of the i^{th} wire (CP) on the j^{th} CP and defined similar to Eq. (24). Similar to Eq. (21), the average electric current in each wire I_i can be expressed as:

$$I_{avg,ik} = sign(df_{i,k}) * \frac{|df_{i,k}| - df_{\min,k}}{df_{\max,k} - df_{\min,k}} \quad (30)$$

$$df_{i,k} = fit_k(\boldsymbol{X}_i) - fit_{k-1}(\boldsymbol{X}_i) \quad (31)$$

where $df_{I,k}$ is the variation of the objective function of the i^{th} CP in the k^{th} iteration.

Big Bang-Big Crunch Algorithm

The big bang-big crunch algorithm proposed by Erol and Eksin (2006) consists of two phases: a big bang phase and a big crunch phase. In the big bang phase, solution candidates are randomly distributed within the search space. This randomness is regarded as energy dissipation in nature. The big bang phase is followed by the big crunch phase. The big crunch is a convergence operator by generating the center of mass. Here, the term mass refers to the inverse of the fitness function value. The point representing the center of mass that is denoted by $\boldsymbol{X}_c$ is calculated according to the formula:

$$\boldsymbol{X}_c = \frac{\sum_{i=1}^{N} \frac{1}{fit(i)} x^i}{\sum_{i=1}^{N} \frac{1}{fit(i)}} \quad (32)$$

where x^i is a point within an N-dimensional search space generated, $fit(i)$ is the fitness function value of this point, N is the population size in the big bang phase. When the big crunch phase is completed, the big bang phase is carried out to produce new candidates for the next iteration. These new candidates are produced using a normal distribution around the center of mass of the previous iteration. The standard deviation of this normal distribution decreases as the optimization process proceeds:

$$\boldsymbol{X}_{i,new} = \boldsymbol{X}_c + \frac{r\alpha_1(\boldsymbol{X}_{\max} - \boldsymbol{X}_{\min})}{k+1} \quad i = 1,2,...,n \quad (33)$$

where $\boldsymbol{X}_c$ stands for center of mass, r is a normal random number, α_1 is a parameter limiting the size of the search space and k is the iteration step. These successive bangs and crunches are carried out alternately until a stopping criterion is satisfied. The constraints can be handled using a penalty scheme similar to that of the CSS algorithm.

A Hybrid MCSS-BBBC Algorithm

In this new hybrid algorithm, the center of mass from the BBBC is added to the MCSS algorithm. In other words, the new location of CPs is obtained as:

$$\mathbf{X}_{j,new} = rand_{j1} \cdot k_a \cdot \mathbf{F}_j + rand_{j2} \cdot k_v \cdot \mathbf{V}_{j,old} + rand_{j3} \cdot \mathbf{X}_c + \mathbf{X}_{j,old} \quad (34)$$

in which, $rand_{j3}$ is a random value in the range [-1, +1]. In this hybrid algorithm, the positive advantages of the BBBC algorithm are added to the MCSS. In other words, the new position of agents in the MCSS is obtained by using the forces generated by the other ones and this will guarantee a good exploration for the algorithm. However, applying the center of mass in addition to the above forces will enhance the exploitation ability of the algorithm. As a result, these two concepts will improve the performance of the algorithm without increasing the complexity of the method or the required time for computation.

TEST EXAMPLE

In this paper, in order to assess the performance of the proposed methodology, a finite element model of a double curvature arch dam considering dam-reservoir interaction is presented as shown in Fig. 3. The reservoir is supposed to be full and the foundation is assumed to be rigid to avoid extra complexities that would otherwise arise. The arch dam is treated as a three-

dimensional linear structure and linear dynamic analysis is performed using the Newmark time integration method. Gravity, hydrostatic loads and hydrodynamic loads are involved here. Since the selection of any design earthquake will not affect the optimization process of the proposed methodology, in this research, the N–S record of 1940 El Centro earthquake is selected to apply to the arch dam-reservoir system in the upstream–downstream direction (PEER, 2009) as shown in Fig. 4.

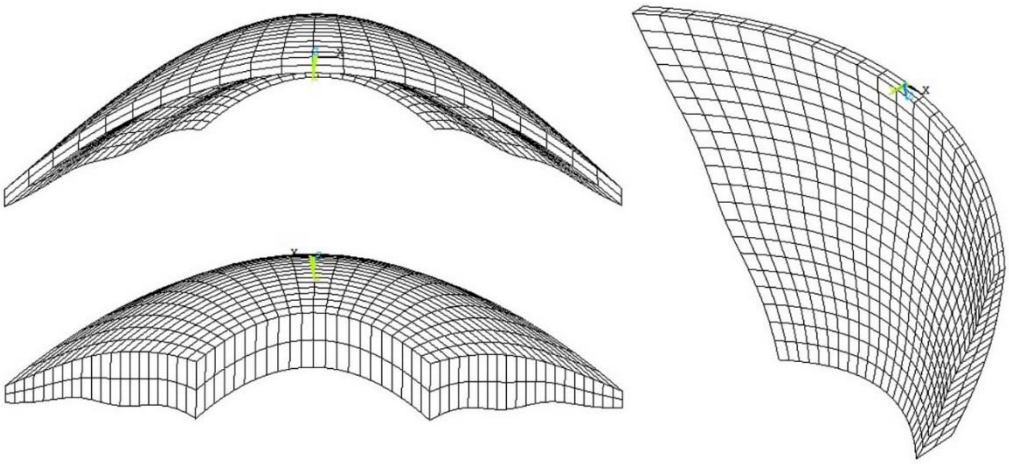

Figure (3): Finite element model of Morrow point dam

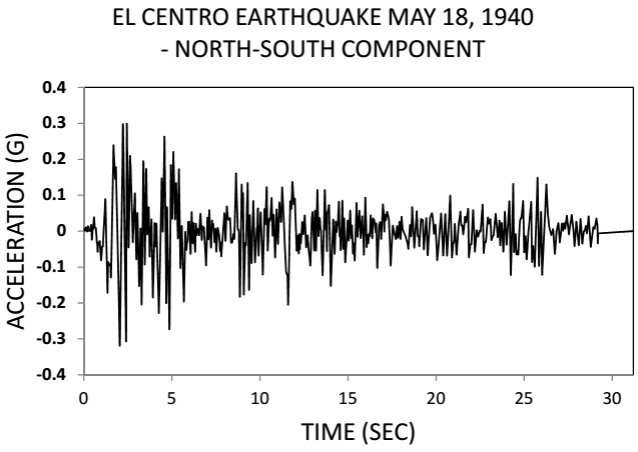

Figure (4): N–S record of 1940 El Centro earthquake

For the example presented in this paper, for all algorithms the number of agents is set to 100 and the number of iterations is limited to 200. The other parameters for the new algorithm are as follows: $k_\alpha = 2$, $k_v = 2$, $\alpha = 1$ and $k_t = 0.75$.

In this example, the optimization of Morrow point arch dam is performed. In order to construct the dam geometry, six controlling levels are considered, so that the dam can be modeled using twenty shape design variables:

$$\mathbf{X}=\{\gamma,\beta,t_{c1},t_{c2},t_{c3},t_{c4},t_{c5},t_{c6},r_{u1},r_{u2},r_{u3},r_{u4},r_{u5},r_{u6},r_{d1},r_{d2},r_{d3},r_{d4},r_{d5},r_{d6}\} \quad (35)$$

The lower and upper bounds of design variables required for the optimization process can be obtained using classic design approaches, as (Varshney, 1982):

$$\begin{aligned}
&0 \le \gamma \le 0.3 && 0.5 \le \beta \le 1 && \\
&3m \le t_{c1} \le 10m && 104m \le r_{u1} \le 135m && 104m \le r_{d1} \le 135m \\
&5m \le t_{c2} \le 14m && 91m \le r_{u2} \le 118m && 91m \le r_{d2} \le 118m \\
&7m \le t_{c3} \le 19m && 78m \le r_{u3} \le 101m && 78m \le r_{d3} \le 101m \\
&9m \le t_{c4} \le 23m && 65m \le r_{u4} \le 85m && 65m \le r_{d4} \le 85m \\
&11m \le t_{c5} \le 26m && 52m \le r_{u5} \le 68m && 52m \le r_{d5} \le 68m \\
&12m \le t_{c6} \le 31m && 39m \le r_{u5} \le 51m && 39m \le r_{d6} \le 51m
\end{aligned} \quad (36)$$

In order to evaluate the performance of the proposed method, the arch dam optimization is performed using the MCSS, BBBC and MCSS-BBBC. In addition, the results are compared to the best answers of three other methods including SPSA, PSO and SPSA-PSO reported in Seyedpoor et al. (2011). All results are listed in Table 2. According to this table, the MCSS performs 2.2% better than SPSA and 4.8% better than PSO. Besides, it is considerable that despite the hybrid SPSA-PSO yields better results than both of the MCSS and BBBC, the MCSS-BBBC outperforms the SPSA-PSO and yields the best answer among six approaches. In Table 3, the best and worst answers of the six methods as well as averages and standard deviations are compared. Numerical results indicate that the solution produced by the new method in terms of both concrete volume and standard deviation is the best.

CONCLUSIONS

A hybrid MCSS-BBBC algorithm for shape optimization of arch dams is proposed. Arch dam geometry is defined employing two polynomials for the central vertical section and two parabolas for the horizontal section. By dividing the dam into five segments along the height, twenty design variables are considered as design parameters. Concrete volume of dam body is considered as the objective function and some geometric, stability and behavioral constraints are involved. Willam-Warnke failure criterion is utilized as behavioral constraint to enforce the resultant principal stresses to stay under a certain limit. The proposed algorithms are applied to optimum design of Morrow point dam as a well-known and real-world double curvature arch dam. In this example, the reservoir is assumed full and hydrodynamic effects of dam-reservoir interaction are taken into account. In addition to gravity and hydrostatic loads, time variant ground acceleration of El Centro earthquake is applied to the numerical model. Results obtained by three metaheuristic algorithms including: MCSS, BBBC and MCSS-BBBC are compared to those of standard SPSA, PSO and SPSA-PSO reported in literature. Comparative studies demonstrate the efficiency and computational merits of the proposed methodology for shape optimization of arch dams.

Table 2. Optimum design of the arch dam obtained by different methods

	(Seyedpoor et al., 2011)			Present work		
Variable	**SPSA**	**PSO**	**SPSA-PSO**	**MCSS**	**BBBC**	**MCSS-BBBC**
$\gamma(m/m)$	0.3000	0.3000	0.3000	0.1310	0.2900	0.1530
$\beta(m/m)$	0.6600	0.5000	0.7400	0.5380	0.5170	0.5150
$tc_1(m)$	5.6300	4.9900	3.7900	5.5070	6.8300	4.6760
$tc_2(m)$	5.7500	5.0000	5.5700	11.0850	10.1710	9.2040
$tc_3(m)$	11.9000	11.6200	11.1800	13.6250	12.1840	13.4340
$tc_4(m)$	16.3300	15.8000	15.1500	15.2930	18.8490	15.3960
$tc_5(m)$	19.8800	20.0000	20.0000	14.6920	21.8720	15.5930
$tc_6(m)$	32.4800	28.7100	34.7900	14.6300	22.1090	15.6670
$ru_1(m)$	100.8400	112.5100	112.3200	108.1620	121.4820	110.4800
$ru_2(m)$	99.8800	108.3700	110.3900	93.7850	112.2860	94.9810
$ru_3(m)$	84.7200	87.3900	93.4700	80.0910	90.8560	80.7300
$ru_4(m)$	65.5700	70.8200	76.9400	68.3960	79.1230	68.4730
$ru_5(m)$	50.4200	59.0600	48.4900	54.1210	59.5240	56.7880
$ru_6(m)$	41.2700	41.1500	41.4300	40.2910	49.3880	41.2770
$rd_1(m)$	99.4700	100.0000	100.0200	107.9120	121.1120	110.1680
$rd_2(m)$	91.8400	87.6800	99.1800	92.6780	97.8820	93.0660
$rd_3(m)$	78.3200	77.5800	88.1371	80.3580	90.9010	80.6230
$rd_4(m)$	63.8500	64.4800	75.0749	66.7040	79.3100	67.4450
$rd_5(m)$	49.0800	52.2000	46.6437	53.9090	56.6850	56.5240
$rd_6(m)$	36.3700	35.9200	33.3125	40.1450	49.4980	40.4990
Concrete volume	240000	246000	228000	234711	267137.5	225576.4

Table 3. Comparison of six different techniques

Volume (e+05) (m^3)	**SPSA**	**PSO**	**SPSA-PSO**	**MCSS**	**BBBC**	**MCSS-BBBC**
Best	240	246	228	234	267	225
Worst	262	266	245	256	285	240
Average	250	258	238	248	276	232
Standard deviation	8.20	7.51	6.02	5.91	15.62	4.32

REFERENCES

Akbari, J., Ahmadi M. T., and Moharrami, H. (2011). "Advances in concrete arch dams shape optimization." Applied Mathematical Modeling, 35, 3316-3333.

Duron, Z. H., and Hall, J. F. (1988). "Experimental and finite element studies of the forced vibration response of Morrow point dam." Earthquake Engineering and Structural Dynamics, 16, 1021-1039.

Erol, O. K., and Eksin, I. (2006). "A new optimization method: big bang-big crunch." Advances in Engineering Software, 37, 106-111.

Gholizadeh, S., and Seyedpoor, S. M. (2011). "Optimum design of arch dams with frequency limitations." Int. J. Optim. Civil Eng., 1, 1-14.

Halliday, D., Resnick R., and Walker, J. (2008). "Fundamentals of physics." Wiley, New York.

Kaveh, A., and Mahdavi, V. R. (2011). "Optimal design of arch dams for frequency limitations using charged sytem search and particle swarm optimization." Int. J. Optim. Civil Eng., 4, 543-555.

Kaveh, A., and Mahdavi, V. R. (2014). "Colliding bodies optimization for design of arch dams with frequency limitations." Int. J. Optim. Civil Eng., 4, 473-490.

Kaveh , A., Motie Share, M. A., and Moslehi, M. (2013). "Magnetic charged system search: a new meta-heuristic algorithm for optimization." Acta Mechanica, 224, 85-107.

Kaveh, A., and Talatahari, S. (2010, a). "A novel heuristic optimization method: charged system search." Acta Mechanica, 213, 267-289.

Kaveh, A., and Talatahari, S. (2010, b). "Optimal design of skeletal structures *via* the charged system search algorithm." Structural and Multi-disciplinary Optimization, 41, 893-911.

Kaveh, A., and Talatahari, S. (2012, a). "Charged system search for optimal design of frame structures." Applied Soft Computing, 12, 382–393.

Kaveh, A., Talatahari, S., and Farahmand Azar, B. (2012,b). "Optimum design of composite open channels using charged system search algorithm." Iranian Journal of Science and Technology, 36, 67-77.

Kuo, J. S.-H. (1982). "Fluid-structure interactions: added mass computations for incompressible fluid." Earthquake Engineering Research Center, University of California, Berkeley.

PEER. (2009). "El Centro, 1940 ground motion data." In: P. E. E. R. Centre (Ed.).

Seyedpoor, S. M., Salajegheh, J., Salajegheh, E., and Gholizadeh, S. (2011). "Optimal design of arch dams subjected to earthquake loading by a combination of simultaneous perturbation stochastic approximation and particle swarm algorithms." Applied Soft Computing, 11, 39-48.

Tan, H., and Chopra, A. K. (1996). "Dam-foundation rock interaction effects in earthquake response of arch dams." Journal of Structural Engineering, 122, 528-538.

USACE. (2007). "Earthquake design and evaluation of concrete hydraulic structures." U. S. Army Corps of Engineers, Washington, D.C., United States of America.

USBR. (1977). "Design criteria for concrete arch and gravity dams." In: U. S. D. O. I. B. O. Reclamation (Ed.). US Government Printing Office, Washington.

Varshney, R. S. (1982). "Concrete dams." Oxford and IBH Publishing Co., New Delhi.

Willam, K. J., and Warnke, E. P. (1975). "Constitutive model for the triaxial behavior of concrete." In: Proceedings of the International Association for Bridge and Structural Engineering, 1-30.

Zhu, B., Rao, B., Jia, J., and Li, Y. (1992). "Shape optimization of arch dams for static and dynamic loads." J. Struct. Eng., 118, 2996-3015.